



Thermal and Morphological Studies on Bismaleimide Modified ZnO Nanoparticles

M. VADIVEL¹, M. SURESH CHANDRA KUMAR^{1,*}, V. SELVAM¹, SUTHA SHOBANA² and S. ARVIND NARAYAN³

¹Polymer Nanocomposite Centre, Department of Chemistry & Research Centre, Scott Christian College, Nagercoil-629 003, India

²Department of Chemistry, Rajas Institute of Technology for Women, Ozhuginasari, Nagercoil-629 001, India

³Faculty of Science and Humanities K.N.S.K. College of Engineering, Therekalpathoor, Nagercoil-629 901, India

*Corresponding author: E-mail: vadivelche@rediffmail.com

Received: 17 October 2013;

Accepted: 6 January 2014;

Published online: 30 September 2014;

AJC-16093

The bismaleimide (N,N'-bismaleimide-4,4'-diphenylmethane) (BMI) modified siliconized zinc oxide nanoparticles were prepared in chloroform. The FT-IR spectroscopy analysis of BMI/ZnO reveals that -NH₂ groups of siliconized ZnO reacts with the maleimide double bond of bismaleimide molecules through a nucleophilic (Michael) addition reaction. The thermal (TG) and morphological properties of bismaleimide modified zinc oxide nanoparticles (BMI/ZnO), were investigated. The particle size and morphology of zinc oxide nanoparticles and siliconized zinc oxide nanoparticles were determined by XRD. The SEM images indicate that the diameter of the zinc oxide nanoparticles is in the range of 25-40 nm with a strong aggregation process. It is observed that aggregates of bismaleimide modified siliconized zinc oxide nanocomposites of different size and shape are heterogeneously distributed in the elastomeric surface due to the low shear stress and processing time, which do not make an exfoliated material.

Keywords: Bismaleimide modified zinc oxide nanoparticles, FT-IR, XRD, TG, SEM.

INTRODUCTION

Nanoparticles and composites show very interesting physical properties and lead a ground-breaking class of materials for the development of novel devices, which have a broad range of applications. In particular composites of inorganic in polymer matrices have been proven to be inorganic nanoparticles and the flexibility offered by the polymer host¹. In recent years, the II-VI semiconductor zinc oxide (ZnO nanoparticles) nanostructures have drawn many attentions in the fabrication of efficient material in different fields with many extraordinary properties, including nontoxicity, biological compatibility, chemical and photochemical stability, high electrochemical activities and easy preparation *etc.*^{2,3}. Various fabrication strategies are adapted for nanoscaled ZnO preparation, such as precipitation⁴, thermal decomposition⁵ and electro deposition⁶. Zinc oxide nanostructures are traditionally known as a wide band gap (3.36 eV) with an excitation binding energy (60 meV) larger than its thermal energy which ensures an efficient ultraviolet-blue emission (26meV) at room temperature⁷. It has a wide range of potential applications in various devices such as UV lasers, solar cells high sensitivity chemical gas or volatile organic compound sensors and DNA sequence sensors varsities displays, *etc.* due to its electrical, optoelectronic and photochemical properties⁸. Zinc oxide

nanoparticle is also a bio-safe and biocompatible material and can be directly used for biomedical applications without coating⁹. Particle surface modification is regarded as an effective way to restrain the ultra-fine particles high oxidative and photochemical catalytic activities¹⁰. Zinc oxide nanoparticles were grafted by aminopropyltriethoxysilane (APTES) in various conditions in order to compare the properties of coated and non-coated powders¹¹.

Bismaleimides (BMI) are broadly used as high performance composite matrices in aerospace industry. As compared with other thermosetting polyimides, bismaleimides display both excellent high performance and low cost¹². Silica-BMI composite found that the materials could be used as an alternative to the broadly used silica-epoxy composite¹³. Nanosilica-BMI based composite materials are the potential solutions to overcome the limitations and demands in the field of semiconductor packaging¹⁴. Silica-BMI nanocomposite with the modification of silica surface with organo-functional groups. Studies revealed the grafting of epoxide groups onto the silica surface¹⁵. In this study, we explored the grafting of maleimide rings which was achieved by reacting amine-grafted zinc oxide nanoparticles with BMI (BMI/ZnO) and were prepared. The structural, thermal and morphological properties were investigated using FT-IR, TG, XRD and SEM.

EXPERIMENTAL

4,4-Diphenyl methane was purchased from Ciba-Geigy Ltd., Mumbai, India. γ -Aminopropyltriethoxysilane (γ -APTS), a grafting agent was supplied by Aldrich, USA. Zinc acetate dihydrate was purchased from Central Drug House Pvt. Ltd, India. Dibutyltindilaurate (DBTDL), was obtained from Merck. Maleicanhydride was purchased from Otto Kemi, India. Nickel acetate was supplied by HiMedia Laboratories Pvt. Ltd, India. Triethyl amine was purchased from Fisher Chem Ltd, India.

Synthesis of zinc oxide nanoparticles (ZnO NPs): 0.2194 g (1 m mol) Zinc acetate dihydrate and 40 g ethanol were taken in a 250 mL round-bottom flask fitted with a condenser and the mixture was refluxed at 50 °C for 1 h using magnetic stirrer. Ethanol solution of NaOH (0.08 g NaOH dissolved in 5 mL ethanol) was added slowly to the reaction mixture under constant stirring. The reaction was allowed to stand for 6 h, after the complete addition of ethanol solution. The clear aqueous solution turned into a dirty white colloid without any precipitation. The colloidal solution was centrifuged, zinc oxide nanoparticles was collected and dried under vacuum at 110 °C for 2 h.

Synthesis of siliconized zinc oxide nanoparticles (SiZnO NPs): 2 g of zinc oxide nanoparticles was taken in a 250 mL three necked, round-bottom flask fitted with a condenser and nitrogen flow. 200 mL of anhydrous toluene was added and the suspension was stirred for 1 h. 1 mL of γ -Aminopropyltriethoxysilane (γ -APTS) was added gradually. The reaction mixture was refluxed for 15 h and then filtered. Excess APTS was removed by washing with fresh toluene and dried under vacuum at 110 °C for 2 h to remove toluene (**Scheme-I**).

Synthesis of bismaleimide (BMI): Synthesis of bismaleimide was carried out in a 1 L three necked flask equipped with mechanical stirrer, reflex condenser and nitrogen inlet. 0.5 mole diaminodiphenylmethane was dissolved in 600 mL of acetone in the flask. Powdered maleic anhydride (98.1 g, 1 mol) was added in portions. An exothermic reaction was observed and the stirring was continued for 1 h to complete the reaction. A bright yellow precipitate of bismaleimic acid was obtained. The precipitate was filtered in a G4 sintered crucible, washed well with copious amount of toluene and dried in vacuum. The yellow bismaleimic acid powder was dissolved in 200 mL of acetone. Nickel acetate (1 g) and triethylamine (28 mL) were added to the solution and the entire

mixture was heated slowly to reflux. Acetic anhydride (117.9 mL) was added to the reaction mixture by means of pressure equalizing funnel and heating was continued for another 3 h. The resulting yellowish brown solution was added in drops to large quantities of crushed ice with efficient stirring. The resulting yellow coloured bismaleimide (N,N'-bismaleimide-4,4'-diphenylmethane) was separated by filtration, washed with copious amount of ice-cold distilled water, recrystallized from toluene and vacuum dried at 80 °C for 5 h (**Scheme-II**).

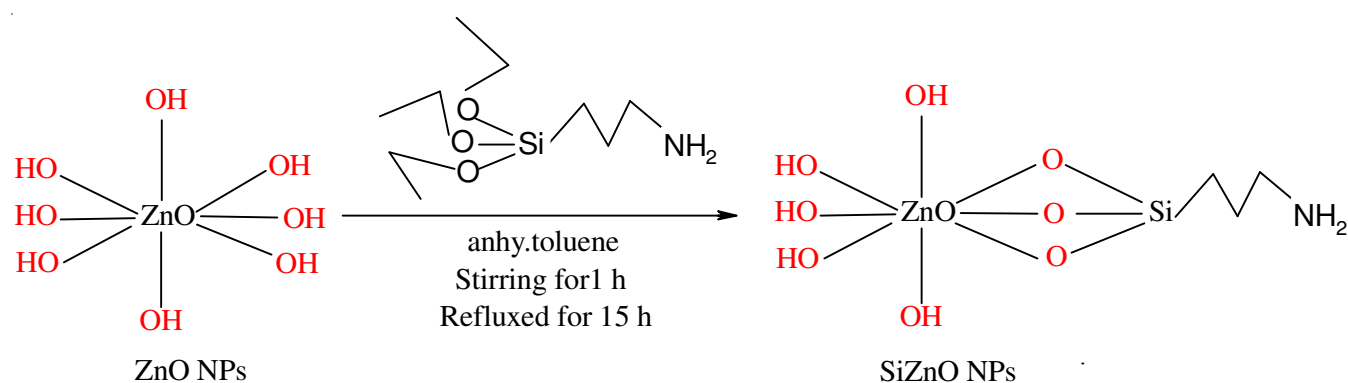
Synthesis of bismaleimide modified zinc oxide nanoparticles (BMI/ZnO NPs): 2 g of Siliconized zinc oxide nanoparticles was mixed with 4 g of BMI powder (molar excess). 50 mL of chloroform was added to the mixture and was agitated for 24 h using a magnetic stirrer. The sample was then separated from the liquid phase by centrifugation at 3000 rpm and washed thoroughly with chloroform (3 times) and acetone (twice). The sample was dried at 80 °C to remove chloroform (**Scheme-II**).

Characterization: The FT-IR spectra were recorded on a Shimadzu-1800S spectrophotometer with KBr pellets for solid samples. The viscous liquid samples were directly applied by dubbing on a KBr pellet. Thermal stabilities were recorded in dynamic nitrogen atmosphere (flow rate 20 cm³/min) with a heating rate of 10 K/min using a Perkin Elmer (TGS-2 model) thermal analyzer. Powder X-ray diffraction patterns were recorded with on Bruker AXS D8 advance powder X-ray diffractometer. Scanning Electron Micrography with Energy Dispersive Spectrometry associated (SEM/EDS) using JSM-5610 scanning electron microscope was used for morphological evaluation.

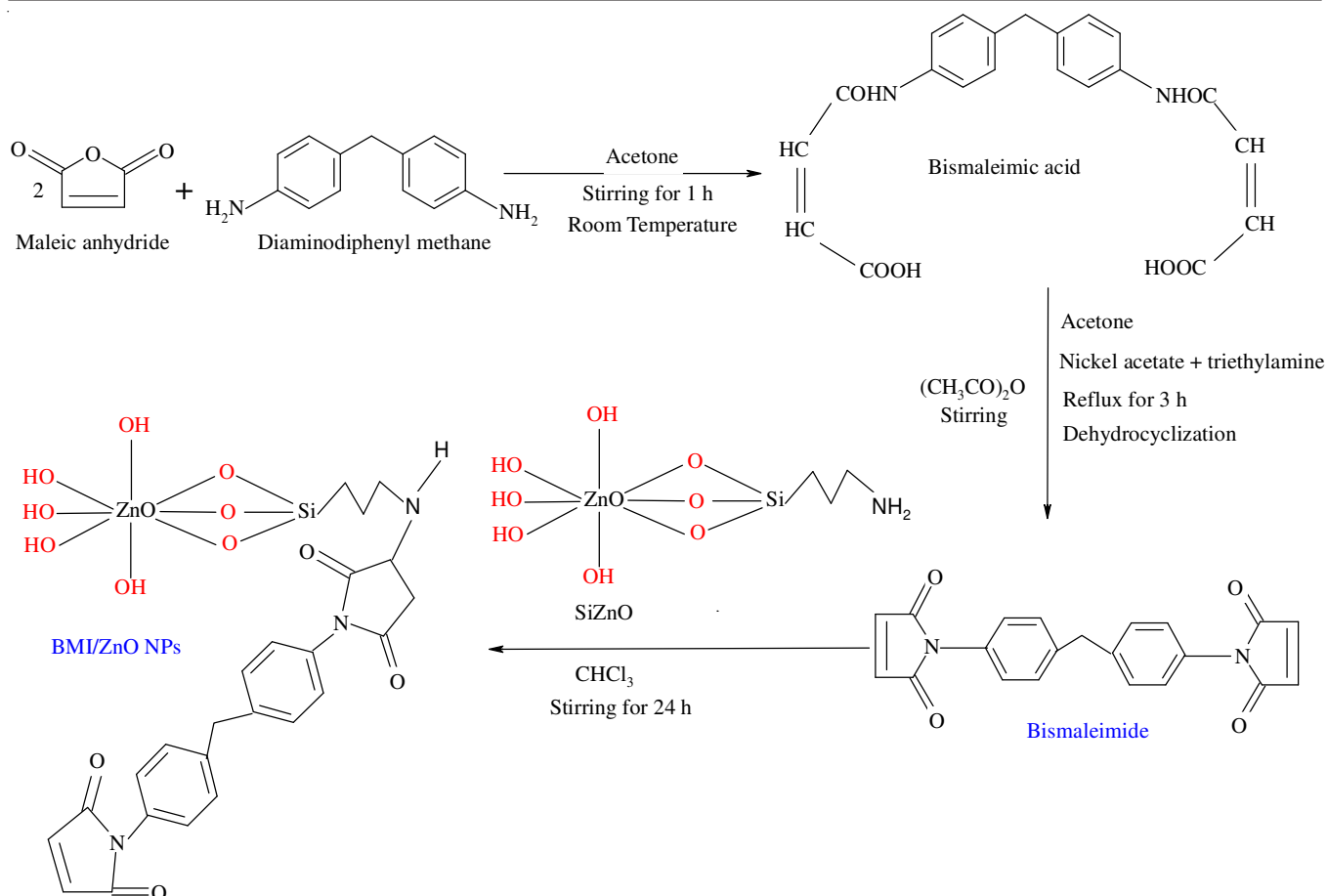
RESULTS AND DISCUSSION

FT-IR spectra: From vibrational spectra of ZnO nanoparticles, Zn-O stretching vibration at 424.15 cm⁻¹, O-H stretching frequency at 3458 cm⁻¹ and O-H bending frequency at 937.44 cm⁻¹ were found. The FT-IR spectra are depicted in Fig. 1.

The spectra of SiZnO nanoparticles show that Zn-O stretching vibration at 424.35 cm⁻¹, O-H stretching vibration at 3417.98 cm⁻¹ and C-H stretching vibration at 2926.11 cm⁻¹. Reiteration of characteristic peak of zinc oxide nanoparticle and observation of a sharp and strong Si-O asymmetric stretching frequency (1012.66 to 1116. cm⁻¹) for surface-modified (siliconized) sample indicates that the main structure of zinc



Scheme-I: Synthesis of SiZnO nanoparticles



Scheme-II: Synthesis of Bisaleimide and BMI/ZnO nanoparticles

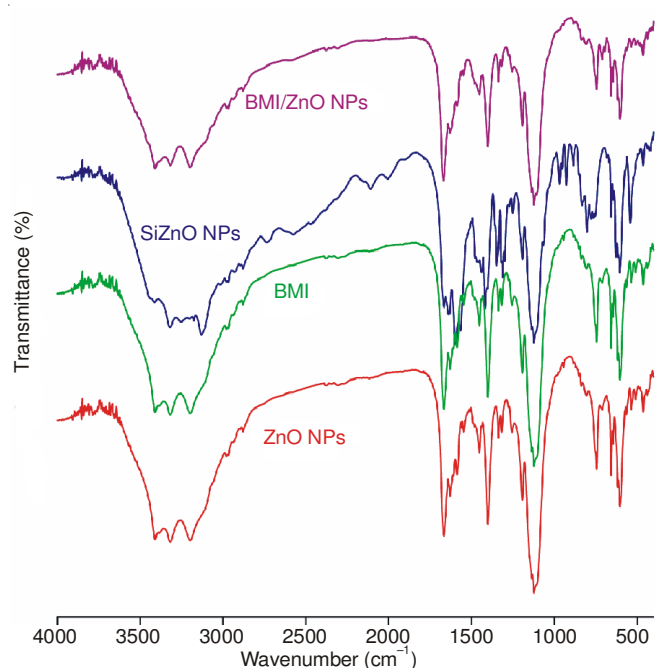


Fig.1. FTIR of ZnO, BMI, SiZnO nanoparticles and BMI/ZnO nanoparticles

oxide nanoparticle is not altered by silane encapsulation. The O-H bending vibration at 937.44 cm^{-1} , due to the hydroxyl groups attached to the surface of ZnO, was not observed for SiZnO, confirms the condensation reaction between the surface -OH groups of ZnO nanoparticles and $-\text{OCH}_2\text{CH}_3$ groups of

γ -APTS. This also suggests that the modification reactions occurred primarily on the ZnO nanoparticles surface rather than in the internal structure. However, silane treatment results increase of peak intensity at 3417.98 cm^{-1} which is ascribed to the overlapping of -NH stretching frequency of the aminosilane with OH stretching frequency. The appearance of new peak at 1745.84 cm^{-1} (-NH bending vibration of amine group) further supports the above fact.

From FT-IR spectrum of BMI, cyclic imide-C=O stretching vibration at 1707.06 cm^{-1} , cyclic -C=O bending vibration at 732.98 cm^{-1} , C-N stretching vibration at 1359.16 cm^{-1} and aromatic -C=C- stretching frequency at 1627.99 cm^{-1} . The characteristic absorptions due to =C-H stretching vibration of maleimide at 3090.10 cm^{-1} , =C-H bending vibration of maleimide moiety at 689.2 cm^{-1} and =C-H out-of-plane bending of maleimide at 832.4 cm^{-1} are widely accepted as a reference to follow the conversion of BMI double bonds^{16,17}.

The FT-IR spectrum of BMI/ZnO nanoparticles reveals the absorption peaks due to =C-H bending at 689.2 cm^{-1} and =C-H out-of-plane bending at 832.4 cm^{-1} of maleimide monomer disappeared during the BMI/ZnO nanoparticles formation, suggesting the cure of maleimide group. Two additional peaks observed for BMI modified ZnO nanoparticles, -C=O stretching frequency at 1714.72 cm^{-1} and aromatic -C=C- stretching frequency at 1612.19 cm^{-1} , compared to the siliconized ZnO nanoparticles, indicates the presence of BMI molecules on the surface of the siliconized ZnO nanoparticles. In addition, the carbonyl peak observed for BMI modified ZnO nano-

particles was shifted to higher wave number (1714.72 cm^{-1}) compared to neat BMI (absorb at 1707.06 cm^{-1}). The shift indicates that $-\text{NH}_2$ groups of siliconized ZnO nanoparticles reacts with the maleimide double bond of BMI molecules, FT-IR analysis of BMI modified ZnO revealed no signs of transamidation and it is clear that the reaction between amine groups and BMI molecules occurred predominantly through a nucleophilic (Michael) addition reaction¹⁸. Most importantly, the carbonyl peak at 1707.06 cm^{-1} indicates the presence of free maleimide double bonds in the BMI/ZnO nanoparticles.

XRD analysis: The size of zinc oxide nanoparticles and siliconized zinc oxide nanoparticles were investigated by XRD. Fig. 2 shows XRD results of ZnO and SiZnO nanoparticles. The main peaks occurs at $2\theta = 32^\circ$, 34.8° and 36.5° , which correspond to (100), (002) and (101) planes respectively. As shown in the figures, the diffraction peaks of siliconized zinc oxide nanoparticles and zinc oxide nanoparticles are good agreement with that of the hexagonal wurtzite structure, which are consistent with the values in the standard card (JCPDS 36-1451). The average size of zinc oxide and siliconized zinc oxide nanoparticles were determined by means of X-ray line-broadening method using Scherrer equation¹⁹. These results show that the size of zinc oxide nanoparticles was not affected by siliconization and ranged from 25 to 40 nm.

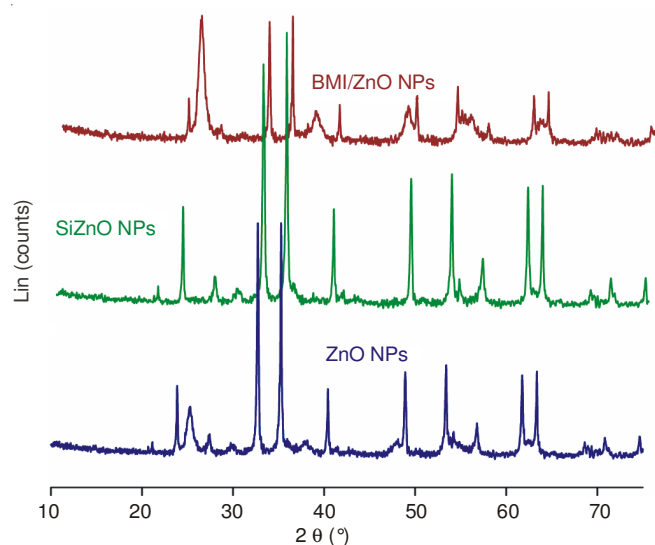


Fig. 2. XRD of ZnO nanoparticles, SiZnO nanoparticles and BMI/ZnO nanoparticles

Thermal analysis: Thermal analysis technique (TG) measures the heat flow change of a material as a function of temperature and is widely used in determining melt temperatures and heat transitions. Fig. 3 represents the thermogram of BMI/ZnO nanoparticles. The thermogram of BMI shows an endothermic melting transition at 154°C and exotherm at 262°C . Also BMI modified ZnO nanoparticles (BMI/ZnO NPs) system revealed a sharp endothermic peak at 225.02°C , associated with melting, followed by exothermic transition due to curing at 264.21°C . The high exothermic peak found at 316.45°C obtained for BMI/ZnO nanoparticles system is due to the following reactions, (i) addition reaction of $-\text{NH}_2$ groups of silane modified ZnO with double bonds of bismaleimide (Michael addition) and (ii) homopolymerization of bismale-

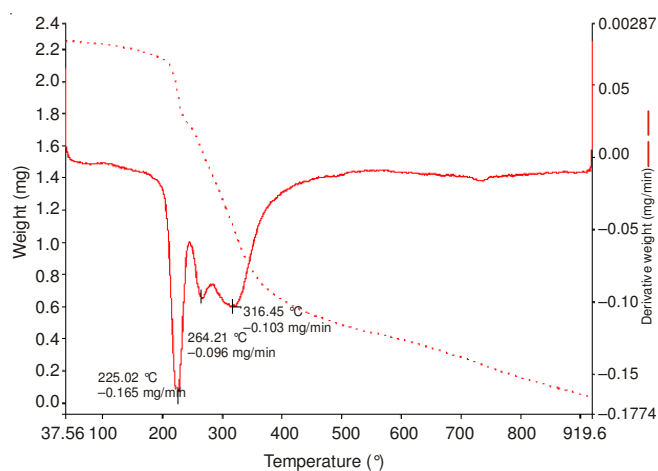


Fig. 3. Thermogram of BMI/ZnO nanoparticles

imide. However, it was reported that the reaction (ii) is least possible due to the higher activation energy (higher temperature) to initiate homopoly-merization of bismaleimide²⁰. For example the temperature required to start the homopolymerization reaction for BMI is 180°C .

Morphological investigation: The SEM images of the zinc oxide nanoparticles and siliconized zinc oxide nanoparticles are displayed in Fig. 4a-b. Zinc oxide nanoparticles shows crystallites and several crystallites are aggregated into one grain. Indeed, as shown in Fig. 4a-b, indicates that the zinc oxide nanoparticles consist of an assembly of ultrafine particles. The diameter of the zinc oxide and siliconized zinc oxide nanoparticles is in the range of 25-40 nm. The SEM micrograph of the unmodified BMI (Fig. 4c) reveals crystallites with micropores indicating brittle phase. The surface of the BMI modified ZnO nanoparticles (Fig. 4d) reveals a heterogeneous morphology due to low shear stress and processing time²¹. The calculations of the average nanoparticle size indicate that the average size remains unchanged by the grafting reaction.

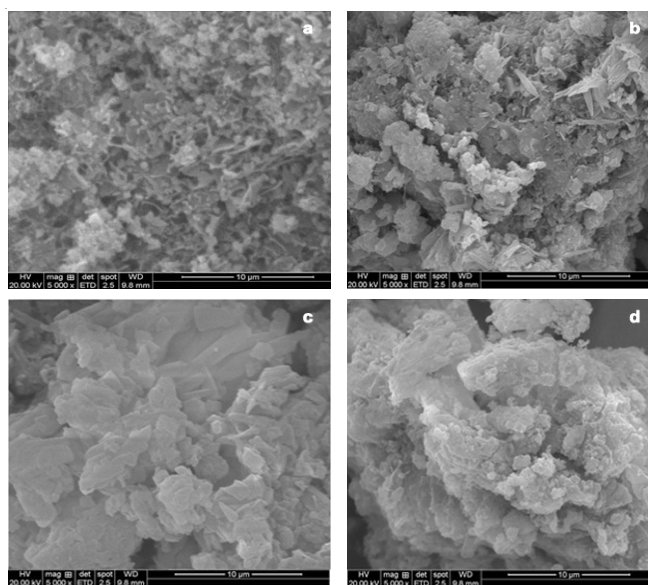


Fig. 4. SEM Pictogram for (a) ZnO nanoparticles (b) SiZnO nanoparticles (c) BMI (d) BMI/ZnO nanoparticles

Conclusion

The FT-IR spectrum of synthesized BMI/ZnO nanoparticles shows the chemical reaction between amine groups of siliconized ZnO nanoparticles and BMI through a nucleophilic (Michael) addition reaction. The thermogram of BMI modified ZnO nanoparticles (BMI/ZnO NPs) system shows an endothermic peak at 225.02 °C and an exotherm at 264.210 °C, confirms addition reaction of -NH₂ groups of silane modified ZnO with double bonds of bismaleimide. The XRD and SEM images of the zinc oxide, siliconized ZnO and bismaleimide modified ZnO nanoparticles show nanorods have the diameter in the range of 25-40 nm with strong aggregation. The SEM of BMI modified ZnO nanoparticles indicates a heterogeneous morphology due to low shear stress. The SEM micrograph of the EPDM-R-BMI/ZnO system reveals that the minor component (BMI/ZnO) is dispersed within a continuum of the major component (EPDM) with co-continuous morphology.

REFERENCES

1. P. Liu, *Eng. Aspects*, **291**, 155 (2006).
2. X.L. Zhu, I. Yuri, X. Gan, I. Suzuki and G.X. Li, *Biosens. Bioelectron.*, **22**, 1600 (2007).
3. F.F. Zhang, X.L. Wang, S.Y. Ai, Z.D. Sun, Q. Wan, Z.Q. Zhu, Y.Z. Xian, L.T. Jin and K. Yamamoto, *Anal. Chim. Acta*, **519**, 155 (2004).
4. A.P.A. Oliveria, J.F. Hochepped, F. Grillion and M.H. Berger, *Chem. Mater.*, **15**, 3202 (2003).
5. M. Yin, Y. Gu, I.L. Kuskovsky, T. Andelman, Y. Zhu, G.F. Neumark and S. O'Brien, *J. Am. Chem. Soc.*, **126**, 6206 (2004).
6. T. Pauporte, T. Yoshida, A. Goux and D. Lincot, *Electroanal. J. Chem.*, **534**, 55 (2002).
7. J. Zheng, R. Ozisik and R.W. Siegel, *Polymer*, **46**, 10873 (2005).
8. A.E. Suliman and Y. Tang, *J. Appl. Sci.*, **7**, 314 (2007).
9. M.S.A.S. Shah, M. Nag, T. Kalagara, S. Singh and S.V. Manorama, *Chem. Mater.*, **20**, 2455 (2008).
10. S.G. Hussain, D. Liu, X. Huang, K.M. Sulieman and S.T. Rasool, *Int. J. Nanopart.*, **2**, 443 (2009).
11. F. Grasset, N. Saito, D. Li, D. Park, I. Sakaguchi, N. Ohashi, H. Haneda, T. Roisnel, S. Mornet and E. Duguet, *J. Alloys Comp.*, **360**, 298 (2003).
12. J.A. Parker, D.A. Kowrides, Foblen and G.M. High, Temperature Polymer Matrix Composites. NASA Conf Pub No 2385:5 (1983).
13. K. Albert, B. Pfeleiderer, E. Bayer and R. Schnabel, *J. Colloid Interf. Sci.*, **142**, 35 (1991).
14. J. Meng and X. Hu, *Polymer*, **45**, 9011 (2004).
15. H.M. Kao, Y.Y. Tsai and S.W. Chao, *Solid State Ion.*, **176**, 1261 (2005).
16. K. Krishnan, T.M. Vijayan and K.N. Ninan, *J. Mater. Sci.*, **34**, 5907 (1999).
17. A.A. Kumar, M. Alagar and R.M.V.G.K. Rao, *J. Appl. Polym. Sci.*, **81**, 2330 (2001).
18. G. Shen, A. Horgan and R. Levicky, *Colloids Surf. B*, **35**, 59 (2004).
19. M.T. Weller, Inorganic Materials Chemistry, Oxford Chemistry Primer, 5 (1996).
20. P. Musto, E. Mariuscelli, G. Ragosta, P. Russo and G. Scarinzi, *J. Appl. Polym. Sci.*, **69**, 1029 (1998).
21. Y.W. Lao, S.T. Kuo and W.H. Tuan, *Ceram. Int.*, **35**, 1317 (2009).